FORSCHUNGSZENTRUM JÜLICH GmbH
Zentralinstitut für Angewandte Mathematik
D-52425 Jülich, Tel. (02461) 61-6402

Technical Report

Compact Finite Difference Schemes of Sixth Order for the Helmholtz Equation

Godehard Sutmann

FZJ-ZAM-IB-2005-08

July 2005
(last change: 28.7.2005)

Preprint: submitted for publication

Compact Finite Difference Schemes of Sixth Order for the Helmholtz Equation

Godehard Sutmann[1]

Central Institute for Applied Mathematics (ZAM) and
John von Neumann Institute for Computing (NIC)
Research Centre Jülich (FZJ)
D - 52425 Jülich, Germany

July 20, 2005

[1] g.sutmann@fz-juelich.de

Abstract

New compact finite difference schemes of sixth order are derived for the three dimensional Helmholtz equation, $\Delta u - \kappa^2 u = -f$. Convergence characteristics and accuracy are compared and a truncation error analysis is presented for a broad range of κ-values.

Keywords: Poisson equation, compact solvers, iterative solvers, Padé approximation

1 Introduction

In a variety of physical problems, the solution of a Helmholtz type equation

$$\Delta u(\mathbf{r}) - \kappa^2 u(\mathbf{r}) = \Lambda u(\mathbf{r}) = -f(\mathbf{r}) \qquad , \qquad \mathbf{r} \in \Omega \tag{1}$$

with Dirichlet boundary conditions

$$u(\mathbf{r}_b) = u_0(\mathbf{r}_b) \qquad , \qquad \mathbf{r}_b \in \partial\Omega \tag{2}$$

is required, where u_0 is a predefined value of the field solution on the domain boundary, $\mathbf{r}_b$. For further purposes, the Helmholtz operator $\Lambda = \Delta - \kappa^2$ was introduced. The differential equation appears in a natural way in the solution of the wave equation, in which case $\kappa = i\omega/c_0$ is the wavenumber in a dispersive medium (ω is the wave frequency and c_0 the speed of light or the speed of sound) or in the solution of the linearised Poisson-Boltzmann equation, in which case $\kappa = q\sqrt{8\pi\beta c/\epsilon}$ (q is the charge of an ion, c the ionic concentration, ϵ the dielectric constant of the solvent and β the inverse thermal energy). Due to its importance in this area of research, great effort has been spent to develop fast and accurate methods for solution. In Ref. [1] fourth and sixth order methods were studied. Boisvert formulated extensions of sixth order accuracy for the HODIE method [2]. Alternative schemes were presented by Manohar and Stephenson [3] for fourth and sixth order. Harari and Turkel also presented various fourth order methods for time-harmonic wave propagation [4]. Furthermore, fourth order methods for the Helmholtz equation with constant coefficients on uniform grids were presented in Ref. [5].

In the present paper new sixth order schemes are developed for the finite difference representation of the Laplace operator appearing in the Helmholtz equation with constant coefficients. It partially extends the schemes developed recently for the Poisson equation [6]. One scheme (L_{6c}) is based on a reformulation of higher derivatives, appearing in the Taylor expansion of the discrete form of the field. This representation has the advantage of being fully compact in the case of a differentiable source function f, i.e. it needs only information of the nearest neighbour grid points. Two other sixth order approximations (L_{P04}, L_{P22}) follow from a Padé approximation of the high order finite difference expansion for the Laplace operator. Although these schemes are not fully compact, i.e. they need also next nearest grid points for the solution, it is found that they have better convergence characteristics and a better error reduction for large values of κ. In practical applications, different schemes may be combined, i.e. using good converging schemes in the domain interior and a fully compact scheme on the boundary. In such a way it is also straight forward to incorporate these schemes into a multigrid algorithm. The new finite difference schemes are compared to the sixth order scheme (L_{3bl}) emerging naturally from the finite difference expansion of the Laplace operator.

2 Theory

A straight forward implementation of high order formulations for finite difference schemes is found from the expansion [7]

$$\left.\frac{\partial^2 u}{\partial \alpha^2}\right|_{\alpha=ih_\alpha} = \frac{4}{h_\alpha^2}\left[\sinh^{-1}\left(\frac{\delta_\alpha}{2}\right)\right]^2 \tag{3}$$

$$= \frac{1}{h_\alpha^2}\delta_\alpha^2\left\{1-\frac{1}{12}\,\delta_\alpha^2+\frac{1}{90}\,\delta_\alpha^4-\frac{1}{560}\,\delta_\alpha^6\pm\ldots\right\}u_{i,j,k} \tag{4}$$

A sixth order stencil for the Helmholtz equation is then simply found as

$$\begin{aligned}
\Lambda_{3bl}(000) &: -\frac{49}{6}\frac{1}{h^2}-\kappa^2\\
\Lambda_{3bl}(\pi(1,0,0)) &: \frac{3}{2}\frac{1}{h^2}\\
\Lambda_{3bl}(\pi(2,0,0)) &: -\frac{3}{20}\frac{1}{h^2}\\
\Lambda_{3bl}(\pi(3,0,0)) &: \frac{1}{90}\frac{1}{h^2}
\end{aligned} \tag{5}$$

where $\pi(i,j,k)$ means all permutations of the $(\pm i,\pm j,\pm k)$ arguments. The unpleasant fact of this implementation is that it is a rather extended scheme. For Dirichlet boundary conditions, three layers of grid points have to be prescribed (denoted by the index $3bl$).

The aim here is to derive sixth order compact formulations of the finite difference approximation to Eq.1. A compact form, needing only one boundary layer is derived from a reformulation of higher mixed derivatives. Two other forms, needing two boundary layers, are based on a Padé approximation

$$\mathcal{P}_{m,n}[\partial_\alpha^2 u] = \frac{\sum_{k=0}^{m} a_k x_\alpha^k}{1+\sum_{k=1}^{n} b_k x_\alpha^k} \tag{6}$$

for different sets of m,n.

2.1 Compact reformulation of the Helmholtz equation

In order to find an appropriate description, a Taylor series expansion is performed for the descritized field $u_h \equiv u_{i,j,k}$, where the grid spacing is h. In one spatial direction the expansions in positive and negative direction are

$$u_{i-1,j,k} = u_{i,j,k} - h\partial_x u + \frac{h^2}{2}\partial_x^2 u - \frac{h^3}{6}\partial_x^3 u + \frac{h^4}{24}\partial_x^4 u - \frac{h^5}{120}\partial_x^5 u + \frac{h^6}{720}\partial_x^6 u + O(h^7) \tag{7}$$

$$u_{i+1,j,k} = u_{i,j,k} + h\partial_x u + \frac{h^2}{2}\partial_x^2 u + \frac{h^3}{6}\partial_x^3 u + \frac{h^4}{24}\partial_x^4 u + \frac{h^5}{120}\partial_x^5 u + \frac{h^6}{720}\partial_x^6 u + O(h^7) \tag{8}$$

Adding the two expansions and solving for the second derivative gives

$$\partial_x^2 u = \frac{u_{i-1,j,k} - 2u_{i,j,k} + u_{i+1,j,k}}{h^2} - \frac{h^2}{12}\partial_x^4 u - \frac{h^4}{360}\partial_x^6 u + O(h^6) \tag{9}$$

Therefore the Laplace operator can be approximated in sixth order as

$$\Delta u = \frac{1}{h^2}(\delta_x^2 + \delta_y^2 + \delta_z^2)u - \frac{1}{12}\{\partial_x^4 + \partial_y^4 + \partial_z^4\}u - \frac{h^4}{360}\{\partial_x^6 + \partial_y^6 + \partial_z^6\}u + O(h^6) \tag{10}$$

where $\delta_x^2 u_{i,j,k} \equiv (u_{i-1,j,k} - 2u_{i,j,k} + u_{i+1,j,k})$ was introduced. In the following "$\{.\}$" is used in combination with partial derivatives whereas "$(.)$" is used with finite difference operators.

Eq.10 shows that a sixth order approximation is expressed in terms of derivatives of order four and six of the potential field. The task is therefore to translate these derivatives into compact finite difference operators of high order. These derivatives may be expressed through multiple differentiations of Eq.1, i.e.

$$\{\partial_x^4 + \partial_x^2\partial_y^2 + \partial_x^2\partial_z^2 - \kappa^2\partial_x^2\}\ u = -\partial_x^2 f \tag{11}$$
$$\{\partial_x^2\partial_y^2 + \partial_y^4 + \partial_y^2\partial_z^2 - \kappa^2\partial_y^2\}\ u = -\partial_y^2 f \tag{12}$$
$$\{\partial_x^2\partial_z^2 + \partial_y^2\partial_z^2 + \partial_z^4 - \kappa^2\partial_z^2\}\ u = -\partial_z^2 f \tag{13}$$

from where the fourth derivatives are expressed as

$$\{\partial_x^4 + \partial_y^4 + \partial_z^4\}\ u = -\{\partial_x^2 + \partial_y^2 + \partial_z^2\}\ f - 2\{\partial_x^2\partial_y^2 + \partial_x^2\partial_z^2 + \partial_y^2\partial_z^2\}\ u + \kappa^2\ \{\partial_x^2 + \partial_y^2 + \partial_z^2\}\ u \tag{14}$$

In a similar way expressions for the sixth order and mixed derivatives are derived

$$\begin{aligned}\{\partial_x^6 + \partial_y^6 + \partial_z^6\}u &= -\{\partial_x^2\partial_y^4 + \partial_x^2\partial_z^4 + \partial_y^2\partial_x^4 + \partial_y^2\partial_z^4 + \partial_z^2\partial_x^4 + \partial_z^2\partial_y^4\}u \\ &\quad +\kappa^2\{\partial_x^4 + \partial_y^4 + \partial_z^4\}u - \{\partial_x^4 + \partial_y^4 + \partial_z^4\}f\end{aligned} \tag{15}$$

$$\begin{aligned}\{\partial_x^2\partial_y^4 + \partial_x^2\partial_z^4 + \partial_y^2\partial_x^4 + \partial_x^2\partial_z^4 + \partial_z^2\partial_x^4 + \partial_z^2\partial_y^4\}u &= -\{\partial_x^2\partial_y^2 + \partial_x^2\partial_z^2 + \partial_y^2\partial_z^2\}f \\ &\quad -3\partial_x^2\partial_y^2\partial_z^2 u + \kappa^2\{\partial_x^2\partial_y^2 + \partial_x^2\partial_z^2 + \partial_y^2\partial_z^2\}u\end{aligned} \tag{16}$$

Inserting Eqs.14, 16 into Eq.15 leads to

$$\begin{aligned}\{\partial_x^6 + \partial_y^6 + \partial_z^6\}u &= -\kappa^2\{\partial_x^2 + \partial_y^2 + \partial_z^2\}f + \{\partial_x^2\partial_y^2 + \partial_x^2\partial_z^2 + \partial_y^2\partial_z^2\}f - \{\partial_x^4 + \partial_y^4 + \partial_z^4\}f \\ &\quad +\kappa^4\{\partial_x^2 + \partial_y^2 + \partial_z^2\}u - 3\kappa^2\{\partial_x^2\partial_y^2 + \partial_x^2\partial_z^2 + \partial_y^2\partial_z^2\}u + 3\partial_x^2\partial_y^2\partial_z^2 u\end{aligned} \tag{17}$$

Therefore all derivatives of order four and six in the approximation for the Laplace operator, Eq.10, are expressed in terms of combinations of second derivatives in the spatial directions.

Now the Helmholtz equation is written as a sixth order approximation

$$\frac{1}{h^2}(\delta_x^2 + \delta_y^2 + \delta_z^2)u - \frac{h^2}{12}\{\partial_x^4 + \partial_y^4 + \partial_z^4\}u - \frac{h^4}{360}\{\partial_x^6 + \partial_y^6 + \partial_z^6\}u - \kappa^2 u = -f \tag{18}$$

The expressions of the higher derivatives are inserted into this approximation, leading to

$$\begin{aligned}
&\frac{1}{h^2}(\delta_x^2+\delta_y^2+\delta_z^2)u \\
&+\frac{h^2}{12}\Big[\{\partial_x^2+\partial_y^2+\partial_z^2\}f+2\{\partial_x^2\partial_y^2+\partial_x^2\partial_z^2+\partial_y^2\partial_z^2\}u-\kappa^2\{\partial_x^2+\partial_y^2+\partial_z^2\}u\Big] \\
&+\frac{h^4}{360}\Big[\{\partial_x^4+\partial_y^4+\partial_z^4\}f-\{\partial_x^2\partial_y^2+\partial_x^2\partial_z^2+\partial_y^2\partial_z^2\}f+\kappa^2+\{\partial_x^2+\partial_y^2+\partial_z^2\}f \\
&-\kappa^4\{\partial_x^2+\partial_y^2+\partial_z^2\}u+3\kappa^2\{\partial_x^2\partial_y^2+\partial_x^2\partial_z^2+\partial_y^2\partial_z^2\}u-3\partial_x^2\partial_y^2\partial_z^2u\Big]-\kappa^2u=-f \quad (19)
\end{aligned}$$

This can be reformulated to give

$$\begin{aligned}
&\frac{1}{h^2}(\delta_x^2+\delta_y^2+\delta_z^2)u+\frac{h^2}{6}\left(1+\frac{h^2\kappa^2}{20}\right)\{\partial_x^2\partial_y^2+\partial_x^2\partial_z^2+\partial_y^2\partial_z^2\}u \\
&-\frac{h^4}{120}\partial_x^2\partial_y^2\partial_z^2u-\kappa^2\left(1+\frac{h^2\kappa^2}{12}+\frac{h^4\kappa^4}{360}\right)u \\
=\;&-\left(1+\frac{h^2\kappa^2}{12}+\frac{h^4\kappa^4}{360}\right)f-\frac{h^2}{12}\left(1+\frac{h^2\kappa^2}{30}\right)\{\partial_x^2+\partial_y^2+\partial_z^2\}f \\
&+\frac{h^4}{360}\{\partial_x^2\partial_y^2+\partial_x^2\partial_z^2+\partial_y^2\partial_z^2\}f-\frac{h^4}{360}\{\partial_x^4+\partial_y^4+\partial_z^4\}f \qquad (20)
\end{aligned}$$

where the relation $\{\partial_x^2+\partial_y^2+\partial_z^2\}u=\kappa^2u-f$ was used. The next task is to construct expressions for the finite difference approximations of sixth order for all derivatives of u. These may be constructed again by Taylor expansion. Results are

$$\begin{aligned}
\partial_x^2\partial_y^2\partial_z^2u &= \frac{1}{h^6}\delta_x^2\delta_y^2\delta_z^2 \qquad (21)\\
\{\partial_x^2\partial_y^2+\partial_x^2\partial_z^2+\partial_y^2\partial_z^2\}u &= \frac{1}{h^4}(\delta_x^2\delta_y^2+\delta_x^2\delta_z^2+\delta_y^2\delta_z^2)u \\
&\quad -\frac{h^2}{12}\{\partial_x^2\partial_y^4+\partial_x^2\partial_z^4+\partial_y^2\partial_x^4+\partial_y^2\partial_z^4+\partial_z^2\partial_x^4+\partial_z^2\partial_y^4\}u \\
&= \frac{1}{h^4}(\delta_x^2\delta_y^2+\delta_x^2\delta_z^2+\delta_y^2\delta_z^2)u+\frac{1}{4h^4}\delta_x^2\delta_y^2\delta_z^2u \qquad (22)\\
&\quad -\frac{h^2\kappa^2}{12}\{\partial_x^2\partial_y^2+\partial_x^2\partial_z^2+\partial_y^2\partial_z^2\}u+\frac{h^2}{12}\{\partial_x^2\partial_y^2+\partial_x^2\partial_z^2+\partial_y^2\partial_z^2\}f
\end{aligned}$$

and therefore

$$\begin{aligned}
\{\partial_x^2\partial_y^2+\partial_x^2\partial_z^2+\partial_y^2\partial_z^2\}u &= \left(1+\frac{h^2\kappa^2}{12}\right)^{-1}\Big[\frac{1}{h^4}(\delta_x^2\delta_y^2+\delta_x^2\delta_z^2+\delta_y^2\delta_z^2)u+\frac{1}{4h^4}\delta_x^2\delta_y^2\delta_z^2u \\
&\quad +\frac{h^2}{12}\{\partial_x^2\partial_y^2+\partial_x^2\partial_z^2+\partial_y^2\partial_z^2\}f\Big] \qquad (23)
\end{aligned}$$

Finally one arrives at the expression for the finite difference approximation of the Helmholtz

equation

$$
\begin{aligned}
& \frac{1}{h^2}(\delta_x^2+\delta_y^2+\delta_z^2)u+\frac{1}{6h^2}\left(1+\frac{h^2\kappa^2}{20}\right)\left(1+\frac{h^2\kappa^2}{12}\right)^{-1}(\delta_x^2\delta_y^2+\delta_x^2\delta_z^2+\delta_y^2\delta_z^2)u \\
& +\frac{1}{24h^2}\left[\left(1+\frac{h^2\kappa^2}{20}\right)\left(1+\frac{h^2\kappa^2}{12}\right)^{-1}-\frac{1}{5}\right]\delta_x^2\delta_y^2\delta_z^2u-\kappa^2\left(1+\frac{h^2\kappa^2}{12}+\frac{h^4\kappa^4}{360}\right)u \\
= & -\left(1+\frac{h^2\kappa^2}{12}+\frac{h^4\kappa^4}{360}\right)f-\frac{h^2}{12}\left(1+\frac{h^2\kappa^2}{30}\right)\{\partial_x^2+\partial_y^2+\partial_z^2\}f-\frac{h^4}{360}\{\partial_x^4+\partial_y^4+\partial_z^4\}f \\
& -\frac{h^4}{72}\left[\left(1+\frac{h^2\kappa^2}{20}\right)\left(1+\frac{h^2\kappa^2}{12}\right)^{-1}-\frac{1}{5}\right]\{\partial_x^2\partial_y^2+\partial_x^2\partial_z^2+\partial_y^2\partial_z^2\}f \qquad (24)
\end{aligned}
$$

Eq.24 may be simplified by expanding terms which contain the factor $1/(1+h^2\kappa^2/12)$. Keeping terms up to sixth order, this leads to

$$
\begin{aligned}
& \frac{1}{h^2}(\delta_x^2+\delta_y^2+\delta_z^2)u+\frac{1}{6h^2}\left(1-\frac{h^2\kappa^2}{30}\right)(\delta_x^2\delta_y^2+\delta_x^2\delta_z^2+\delta_y^2\delta_z^2)u \\
& +\frac{1}{30h^2}\delta_x^2\delta_y^2\delta_z^2u-\kappa^2\left(1+\frac{h^2\kappa^2}{12}+\frac{h^4\kappa^4}{360}\right)u \\
= & -\left(1+\frac{h^2\kappa^2}{12}+\frac{h^4\kappa^4}{360}\right)f-\frac{h^2}{12}\left(1+\frac{h^2\kappa^2}{30}\right)\{\partial_x^2+\partial_y^2+\partial_z^2\}f-\frac{h^4}{360}\{\partial_x^4+\partial_y^4+\partial_z^4\}f \\
& -\frac{h^4}{90}\{\partial_x^2\partial_y^2+\partial_x^2\partial_z^2+\partial_y^2\partial_z^2\}f \qquad (25)
\end{aligned}
$$

It is obvious from Eqs.24,25 that the finite difference operators, appearing on the left hand side (*lhs*) are compact. However, on the right hand side (*rhs*) partial derivatives of higher than second order appear. In cases, where the source function f is known and differentiable, this scheme really provides a compact finite difference scheme. In case that f is not differentiable or its analytical form is not known, one also has to approximate the differential operators on the *rhs*. Since partial derivatives of fourth order cannot be simply reduced to combinations of second order derivatives, this gives rise to the inclusion of next nearest neighbour points in the finite difference scheme. The *rhs* of Eq.25 is thereby modified to

$$
\begin{aligned}
& -\left(1+\frac{h^2\kappa^2}{12}+\frac{h^4\kappa^4}{360}\right)f-\frac{h^2}{12}\left(1+\frac{h^2\kappa^2}{30}\right)\{\partial_x^2+\partial_y^2+\partial_z^2\}f-\frac{h^4}{360}\{\partial_x^4+\partial_y^4+\partial_z^4\}f \\
& -\frac{h^4}{90}\{\partial_x^2\partial_y^2+\partial_x^2\partial_z^2+\partial_y^2\partial_z^2\}f\equiv\Gamma_{6c\partial f}f \qquad (26) \\
\rightarrow \quad & -\left(1+\frac{h^2\kappa^2}{12}+\frac{h^4\kappa^4}{360}\right)f-\frac{1}{12}\left(1+\frac{h^2\kappa^2}{30}\right)(\delta_x^2+\delta_y^2+\delta_z^2)f \\
& +\frac{1}{240}\left(1+\frac{h^2\kappa^2}{18}\right)(\delta_x^4+\delta_y^4+\delta_z^4)f-\frac{1}{90}(\delta_x^2\delta_y^2+\delta_x^2\delta_z^2+\delta_y^2\delta_z^2)f\equiv\Gamma_{6c\delta f}f \qquad (27)
\end{aligned}
$$

where the operators $\Gamma_{6c\partial f}$ and $\Gamma_{6c\delta f}$ acting onto the source functions were introduced. In general the present scheme is refered to as L_{6c}. If it is necessary to distinguish between

different cases, the numerical scheme which uses analytical derivatives of the source function will be called henceforth $L_{6c\partial f}$, the one with finite differences $L_{6c\delta f}$.

From Eq.25 and Eq.27 it is easy to obtain a finite difference scheme of fourth order, i.e.

$$\begin{aligned} & \frac{1}{h^2}(\delta_x^2+\delta_y^2+\delta_z^2)u+\frac{1}{6h^2}(\delta_x^2\delta_y^2+\delta_x^2\delta_z^2+\delta_y^2\delta_z^2)u-\kappa^2\left(1+\frac{h^2\kappa^2}{12}\right)u \\ = & -\left(1+\frac{h^2\kappa^2}{12}\right)f-\frac{h^2}{12}\{\partial_x^2+\partial_y^2+\partial_z^2\}f \qquad (28) \\ = & -\left(1+\frac{h^2\kappa^2}{12}\right)f-\frac{h^2}{12}(\delta_x^2+\delta_y^2+\delta_z^2)f+\mathcal{O}(h^4) \qquad (29) \end{aligned}$$

In order to simplify the programming of the scheme, also the stencil notation is given here. The finite difference operator of the *lhs* is given as

$$\begin{aligned} \Lambda_{6c}(000) &: -\frac{64}{15}\frac{1}{h^2}\left(1+\frac{1}{4}h^2\kappa^2+\frac{5}{256}h^4\kappa^4+\frac{1}{1536}h^6\kappa^6\right) \\ \Lambda_{6c}(\pi(1,0,0)) &: \frac{7}{15}\frac{1}{h^2}\left(1+\frac{h^2\kappa^2}{21}\right) \\ \Lambda_{6c}(\pi(1,1,0)) &: \frac{1}{10}\frac{1}{h^2}\left(1-\frac{h^2\kappa^2}{18}\right) \\ \Lambda_{6c}(111) &: \frac{1}{30}\frac{1}{h^2} \end{aligned} \qquad (30)$$

Using finite difference approximations for the *rhs* of Eq.25 the operator $\Gamma_{6c\delta f}$ is given as

$$\begin{aligned} \Gamma_{6c\delta f}(000) &: \frac{67}{120}\left(1+\frac{8}{67}h^2\kappa^2+\frac{1}{201}h^4\kappa^4\right) \\ \Gamma_{6c\delta f}(\pi(1,0,0)) &: \frac{1}{18}\left(1+\frac{h^2\kappa^2}{20}\right) \\ \Gamma_{6c\delta f}(\pi(1,1,0)) &: \frac{1}{90} \\ \Gamma_{6c\delta f}(\pi(2,0,0)) &: -\frac{1}{240} \end{aligned} \qquad (31)$$

In the limiting case of $\kappa \to 0$, Eq.1 is reduced to the Poisson equation. It comes out that the finite difference approximation is

$$\begin{aligned} & \frac{1}{h^2}(\delta_x^2+\delta_y^2+\delta_z^2)u+\frac{1}{6h^2}(\delta_x^2\delta_y^2+\delta_x^2\delta_z^2+\delta_y^2\delta_z^2)u+\frac{1}{30h^2}\delta_x^2\delta_y^2\delta_z^2u \\ = & -f-\frac{h^2}{12}\{\partial_x^2+\partial_y^2+\partial_z^2\}f-\frac{h^4}{90}\{\partial_x^2\partial_y^2+\partial_x^2\partial_z^2+\partial_y^2\partial_z^2\}f \\ & -\frac{h^4}{360}\{\partial_x^4+\partial_y^4+\partial_z^4\}f \qquad (32) \end{aligned}$$

which is the same expression as was obtained in Ref.[8] for the Poisson equation (Note, however, the wrong factor 1/180 in the third term of the *rhs* in that work).

2.2 Padé approximation $\mathcal{P}_{0,4}$

A Padé approximation with $m = 0, n = 4$ of the second partial derivative is given as

$$
\begin{aligned}
(u_{\alpha\alpha})_{ijk} &= \frac{1}{h_\alpha^2}\ \delta_\alpha^2 \left(1 + \frac{1}{12}\ \delta_\alpha^2 - \frac{1}{240}\delta_\alpha^4\right)^{-1} && (33)\\
&= \frac{1}{h_\alpha^2}\ D_{[0,4],\alpha}^{-1} && (34)
\end{aligned}
$$

which leads to the discrete form of the Helmholtz equation

$$
\left\{ \sum_{\alpha=x,y,z} \frac{1}{h_\alpha^2}\ \delta_\alpha^2\ D_{[0,4],\alpha}^{-1} - \kappa^2 \right\} u_{i,j,k} = -f_{i,j,k} \tag{35}
$$

Both sides of Eq.35 can be multiplied by $\prod_{\alpha=x,y,z} D_{[0,4],\alpha}$ and since the operators $D_{[0,4],\alpha}$ commute, Eq.35 is transformed into

$$
\left\{ \sum_{\alpha} \frac{1}{h_\alpha^2}\ \delta_\alpha^2\ D_{[0,4],\beta}\ D_{[0,4],\gamma} \right\} u_{i,j,k} - \kappa^2 \left\{ \prod_{\alpha=x,y,z} D_{[0,4],\alpha} \right\} u_{i,j,k} = -\left\{ \prod_{\alpha=x,y,z} D_{[0,4],\alpha} \right\} f_{i,j,k} \tag{36}
$$

where $\{(\beta,\gamma) \neq \alpha\ \wedge\ \beta \neq \gamma\}$. This is written as

$$
\begin{aligned}
&\left\{ \frac{1}{h^2}(\delta_x^2 + \delta_y^2 + \delta_z^2) + \frac{1}{6h^2}(\delta_x^2\delta_y^2 + \delta_x^2\delta_z^2 + \delta_y^2\delta_z^2) + \frac{1}{48h^2}\delta_x^2\delta_y^2\delta_z^2 \right. && (37)\\
&-\frac{1}{240h^2}\left(\delta_x^2(\delta_y^4 + \delta_z^4) + \delta_y^2(\delta_x^4 + \delta_z^4) + \delta_z^2(\delta_x^4 + \delta_y^4)\right)\\
&-\kappa^2 - \frac{\kappa^2}{12}(\delta_x^2 + \delta_y^2 + \delta_z^2) - \frac{\kappa^2}{144}(\delta_x^2\delta_y^2 + \delta_x^2\delta_z^2 + \delta_y^2\delta_z^2)\\
&\left. +\frac{\kappa^2}{240}(\delta_x^4 + \delta_y^4 + \delta_z^4) \right\} u_{i,j,k}\\
= \quad &-\left\{ 1 + \frac{1}{12}(\delta_x^2 + \delta_y^2 + \delta_z^2) + \frac{1}{144}(\delta_x^2\delta_y^2 + \delta_x^2\delta_z^2 + \delta_y^2\delta_z^2) - \frac{1}{240}(\delta_x^4 + \delta_y^4 + \delta_z^4) \right\} f_{i,j,k}
\end{aligned}
$$

The stencil notation for the Helmholtz operator Λ_{P04} is then given by

$$
\begin{aligned}
\Lambda_{P04}(000) &: -\frac{58}{15}\frac{1}{h^2} - \frac{61}{120}\kappa^2\\
\Lambda_{P04}(\pi(1,0,0)) &: \frac{3}{10}\frac{1}{h^2} - \frac{13}{180}\kappa^2\\
\Lambda_{P04}(\pi(1,1,0)) &: \frac{19}{120}\frac{1}{h^2} - \frac{1}{144}\kappa^2\\
\Lambda_{P04}(111) &: \frac{1}{48}\frac{1}{h^2}\\
\Lambda_{P04}(\pi(2,0,0)) &: \frac{1}{60}\frac{1}{h^2} + \frac{1}{240}\kappa^2\\
\Lambda_{P04}(\pi(1,2,0)) &: -\frac{1}{240}\frac{1}{h^2}
\end{aligned} \tag{38}
$$

and the Γ_{P04}-operator, acting on the source function is given by

$$\begin{aligned}
\Gamma_{P04}(000) &: \frac{61}{120} \\
\Gamma_{P04}(\pi(1,0,0)) &: \frac{13}{180} \\
\Gamma_{P04}(\pi(1,1,0)) &: \frac{1}{144} \\
\Gamma_{P04}(\pi(2,0,0)) &: -\frac{1}{240}
\end{aligned} \tag{39}$$

2.3 Padé approximation $\mathcal{P}_{2,2}$

A second Padé approximation is obtained with $m = 2, n = 2$ and can be written as

$$(u_{\alpha\alpha})_{i,j,k} = \frac{1}{h_\alpha}\ \delta_\alpha^2 D^{(1)}_{[2,2],\alpha}(D^{(2)}_{[2,2],\alpha})^{-1} \tag{40}$$

with

$$D^{(1)}_{[2,2],\alpha} = 1 + \frac{1}{20}\ \delta_\alpha^2 \tag{41}$$

$$D^{(2)}_{[2,2],\alpha} = 1 + \frac{2}{15}\ \delta_\alpha^2 \tag{42}$$

A high order formulation of the discrete Helmholtz equation is then found as

$$\left\{\sum_\alpha \frac{1}{h_\alpha^2}\delta_\alpha^2\ D^{(1)}_{[2,2],\alpha}\ D^{(2)}_{[2,2],\beta}\ D^{(2)}_{[2,2],\gamma}\right\} u_{i,j,k} - \kappa^2 \left\{\prod_\alpha\ D^{(2)}_{[2,2],\alpha}\right\} u_{i,j,k} = -\left\{\prod_\alpha\ D^{(2)}_{[2,2],\alpha}\right\} f_{i,j,k} \tag{43}$$

As before the sum on the *lhs* is understood for $\{(\beta,\gamma) \neq \alpha\ \wedge\ \beta \neq \gamma\}$. Keeping terms up to sixth order in δ_α^2 on the *lhs* this expression is rewritten in terms of δ_α^2 as

$$\begin{aligned}
&\Big\{\frac{1}{h^2}(\delta_x^2+\delta_y^2+\delta_z^2) + \frac{4}{15h^2}(\delta_x^2\delta_y^2+\delta_x^2\delta_z^2+\delta_y^2\delta_z^2) + \frac{1}{20h^2}(\delta_x^4+\delta_y^4+\delta_z^4) \\
&+\frac{12}{125h^2}\delta_x^2\delta_y^2\delta_z^2 + \frac{1}{150h^2}\left(\delta_x^2(\delta_y^4+\delta_z^4)+\delta_y^2(\delta_x^4+\delta_z^4)+\delta_z^2(\delta_x^4+\delta_y^4)\right) \\
&-\kappa^2 - \frac{2\kappa^2}{15}(\delta_x^2+\delta_y^2+\delta_z^2) - \frac{4\kappa^2}{225}(\delta_x^2\delta_y^2+\delta_x^2\delta_z^2+\delta_y^2\delta_z^2)\Big\}\ u_{i,j,k} \\
= \quad &-\Big\{1 + \frac{2}{15}(\delta_x^2+\delta_y^2+\delta_z^2) + \frac{4}{225}(\delta_x^2\delta_y^2+\delta_x^2\delta_z^2+\delta_y^2\delta_z^2)\Big\}\ f_{i,j,k}
\end{aligned} \tag{44}$$

The stencil notation for the Helmholtz operator Λ_{P22} is then given by

$$\begin{aligned}
\Lambda_{P22}(000) &: -\frac{421}{150}\frac{1}{h^2} - \frac{31}{75}\kappa^2 \\
\Lambda_{P22}(\pi(1,0,0)) &: \frac{2}{15}\frac{1}{h^2} - \frac{14}{225}\kappa^2 \\
\Lambda_{P22}(\pi(1,1,0)) &: \frac{8}{75}\frac{1}{h^2} - \frac{4}{225}\kappa^2 \\
\Lambda_{P22}(111) &: \frac{4}{75}\frac{1}{h^2} \\
\Lambda_{P22}(\pi(2,0,0)) &: \frac{7}{300}\frac{1}{h^2} \\
\Lambda_{P22}(\pi(1,2,0)) &: \frac{1}{150}\frac{1}{h^2}
\end{aligned} \tag{45}$$

The Γ_{P22}-operator, acting on the source function is given by

$$\begin{aligned}
\Gamma_{P22}(000) &: \frac{31}{75} \\
\Gamma_{P22}(\pi(1,0,0)) &: \frac{14}{225} \\
\Gamma_{P22}(\pi(1,1,0)) &: \frac{4}{225}
\end{aligned} \tag{46}$$

2.4 Combination of different schemes

It is obvious that the sixth order schemes may have problems at the domain boundaries. In fact, using finite differences for the higher derivatives of the source function in L_{6c}, Eq. 26, one needs two boundary layers in order to evaluate them properly. This can be avoided when the source function is differentiable and one does not need a finite difference prescription, Eq. 26. The two Padé schemes suffer the same deficiency on the boundary. In this case also the Λ-operators need information from the next nearest grid points, which introduces problems at the boundaries.

For differentiable source functions, these problems may be avoided by a combination of different solvers in the relaxation process. E.g. Padé approximations may be used in the interior of the domain, while points close to the boundary are treated by L_{6c}, leading to the schemes $L_{P04/6c\partial f}$ and $L_{P22/6c\partial f}$. Also combinations of $L_{6c\partial f}$ and $L_{6c\delta f}$ are possible, called $L_{6c\delta f/6c\partial f}$. In the case, where no analytically differentiable source functions exist, e.g. stochastic distributions, one has to switch to asymmetric stencils of high order. The latter case will be not considered here but the combinations $L_{6c\delta f/6c\partial f}$, $L_{P04/6c\partial f}$ and $L_{P22/6c\partial f}$ will be examined in Sec. 3.

3 Results

3.1 Convergence and Accuracy

All four finite difference schemes, $L_{3bl}, L_{6c}, L_{P22}, L_{P04}$ were applied to different test cases (cmp. Sec. 3.3). A standard Gauss-Seidel relaxtion scheme was applied for the iterations. One measure for the convergence of the schemes is the ratio of residue norms

$$r_c = \lim_{n\to\infty} \frac{\|\mathbf{r}^{(n)}\|}{\|\mathbf{r}^{(n-1)}\|} \tag{47}$$

where n is the iteration number and the residue norm is defined as the 2-norm

$$\|\mathbf{r}^{(n)}\| = \sqrt{\frac{1}{N}\sum_{i,j,k}\left(\Lambda_{i,j,k}u^{(n)}_{i,j,k} + f_{i,j,k}\right)^2} \tag{48}$$

and $u^{(n)}_{i,j,k}$ is the value of the field after n iterations. This is of course an ideal representation which does not take into account round-off errors, which finally lead for very large n to a saturation in the reduction of the residuum. On the other hand the convergence may also be measured by calculating the spectral radius $\rho(\mathbf{C})$ of the iteration matrix $\mathbf{C}$ of the numerical scheme. For large grids the latter method is however very demanding in memory and is therefore not employed here. It was found however that for $\kappa = 0$ results obtained from residuum norms and spectral radii agree very well on the smaller grids [6]. Of course, the smaller r_c the better the convergence. Convergence rates were calculated for various values of κ by the residuum method. Since this method should give the same results as a calculation of the spectral radius, which is independent of the problem at hand, also the results for r_c should be representative for any chosen problem with a specified value for κ.

In Fig. 1 results for r_c are shown for the finite difference schemes applied on grids with spacings $h = 1/32$ and $h = 1/64$. It is seen that for imaginary κ the convergence becomes worse for all numerical schemes, leading to instabilities of the solution from $\kappa \approx i6$. On the other hand the convergence rate improves strongly when increasing κ to positive values.

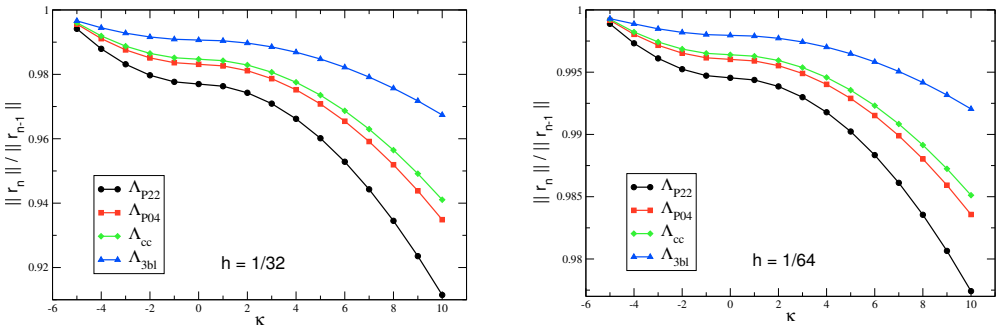

Figure 1: Reduction factor of the residuum norm for operators Λ_{3bl}, Λ_{6c}, Λ_{P04} and Λ_{P22} as function of the parameter κ (negative values of κ represent imaginary values).

λ_{min} ($\times 10^{-2}$)				
κ	Λ_{3bl}	Λ_{6c}	Λ_{P04}	Λ_{P22}
$i5$	1.271	0.425	0.389	0.298
$i2$	1.784	0.937	0.901	0.809
0	1.881	1.035	0.998	0.907
2	1.979	1.133	1.096	1.005
5	2.491	1.646	1.608	1.517

Table 1: Minimum eigenvalue λ_{min} of the stencil matrices $h^2\Lambda_{3bl}$, $h^2\Lambda_{6c}$, $h^2\Lambda_{P04}$ and $h^2\Lambda_{P22}$ determining the residuum reduction in each iteration for Test Case 1 on a grid with $h = 1/64$.

This may be understood from the wave equation analogy, where an imaginary κ corresponds to propagating waves while a real value of κ corresponds to evanescent waves. The latter case gives rise to a very much smoother solution than the former case, leading to a better and faster convergence.

From Fig. 1 it is clearly seen that the different schemes obey strong differences in convergence characteristics. Best convergence is found for the Padé scheme Λ_{P22}, while slowest convergence is found for the scheme with largest extend, Λ_{3bl}.

Another measure of convergence rate can be given in terms of the error norm $\|\mathbf{u}_h^{(n)} - \mathbf{u}_h^{(ex)}\|$, where $\mathbf{u}_h^{(n)}$ is the field solution after n iteration steps and $\mathbf{u}_h^{(ex)}$ is the exact solution of the problem. For large n this gives the discretization error $\|\boldsymbol{\epsilon}_h\|$. The error norm may be estimated by [6]

$$\|\mathbf{u}_h^{(n)} - \mathbf{u}_h^{(ex)}\| \leq \|\boldsymbol{\Lambda}_h^{-1}\mathbf{r}_h^{(n)}\| + \|\boldsymbol{\epsilon}_h\| \tag{49}$$

$$\approx \frac{h^2}{|\lambda_{min}|}\|\mathbf{r}_h^{(n)}\| + \|\boldsymbol{\epsilon}_h\| \tag{50}$$

Here, λ_{min} is the smallest eigenvalue of the stencil matrix $h^2\boldsymbol{\Lambda}_h$. Therefore, the smaller the eigenvalue λ_{min}, the faster the convergence towards the discretization error. Values for λ_{min} for grids with $h = 1/64$ are shown in Table 1. Results for this estimate of the error reduction are shown in Fig. 2 for the $\mathcal{P}[2,2]$ scheme for different grid sizes and $\kappa = 5$, from where a very good correspondence is found.

Another characteristic quantity of the stencils is the discritization error which is described by the error norm $\|\boldsymbol{\epsilon}_h\|$. This quantity is found empirically by solving test cases. As an example, values for $\|\boldsymbol{\epsilon}_h\|$ are shown in Table 2 for the stencils on a grid with mesh size $h = 1/64$. As an interesting fact it is found that $\|\boldsymbol{\epsilon}_h\|$ is reduced for all stencils with increasing κ except for the scheme L_{6c}. This behavior is illustrated also in Fig.1 where results for L_{6c} and L_{P22} are compared for a set of κ-values. This phenomenon can be explained by the expansion of the operators in terms of h. As is shown in Appendix B this scheme has an expansion, which depends on κ^2. Therefore, with increasing κ, the discretization error increases as well. This tendency is not that dramatic when considering imaginary values for κ. This kind of κ-dependence of the discretization error makes it attractive to choose a given finite difference scheme according to the value of κ. From an eigenvalue calculation it is, however, obvious that for values $\kappa > i\sqrt{3}$ the Λ-operator becomes indefinite for which

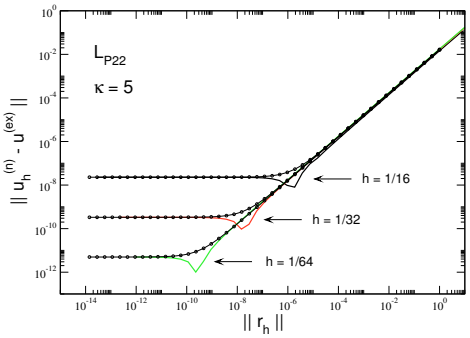

Figure 2: Convergence behavior of the solver L_{P22} towards the discretization error $\|\boldsymbol{\epsilon}_h\|$, applied to Test Case 1 with $\kappa = 5$ for different grid sizes. Compared to the numerical results is the model, Eq. 50, based on an eigenvalue calculation of the stencil matrix Λ_{P22}.

elliptic methods are not appropriate anymore. As is seen in Fig. 1 the value of residuum reduction increases towards the value of 1 for larger imaginary values of κ. For $\kappa \approx i6$ the solution of all operators tend to become unstable ($r_c \geq 1$). This is also the reason why an increase of the discretization error is observed for larger imaginary values of κ in the case of L_{6c}. This fact, however, is also true for the continuous problem, which means that it is a principal problem, not a numerical one, related to the current approximation scheme.

In addition to the schemes, derived in Sec. 2, combinations were explored in order to provide a method, which is able to cope with boundary conditions, prescribed only on one layer of grid points. For Test Case 1 (cmp. Sec. 3.3), the schemes $L_{6c\delta f}$, L_{P04} and L_{P22} were applied in the interior of the computational domain, while $L_{6c\partial f}$ was used at the outermost part of the domain to treat the boundary conditions. These schemes are referred to as $L_{6c\delta f/6c\partial f}$, $L_{P04/6c\partial f}$ and $L_{P22/6c\partial f}$. As is seen in Table 2, the accuracy of the combined schemes is mainly conserved. Only for largest imaginary value of κ it

	$\|\boldsymbol{\epsilon}_h\|$ $(\times 10^{-12})$							
κ	L_{3bl}	$L_{6c\partial f}$	$L_{6c\delta f}$	$L_{6c\delta f/6c\partial f}$	L_{P04}	L_{P22}	$L_{P04/6c\partial f}$	$L_{P22/6c\partial f}$
$i5$	24.6	79.9	37.4	49.1	9.17	42.7	13.8	56.5
$i2$	9.18	26.4	3.83	3.90	1.80	10.2	1.85	10.4
0	8.18	24.8	3.64	3.70	1.58	8.90	1.57	9.02
2	7.48	23.5	3.83	3.87	1.37	7.89	1.39	7.94
5	4.89	19.9	7.81	7.72	0.86	4.96	0.84	4.90

Table 2: Discretization error $\|\boldsymbol{\epsilon}_h\|$ for Test Case 1 and different values of κ for discretization schemes L_{3bl}, $L_{6c\partial f}$, $L_{6c\delta f}$, L_{P04} and L_{P22} as well as combinations of different schemes (cmp. Sec. 2.4), which are fully compact, $L_{6c\delta f/6c\partial f}$, $L_{P04/6c\partial f}$ and $L_{P22/6c\partial f}$.

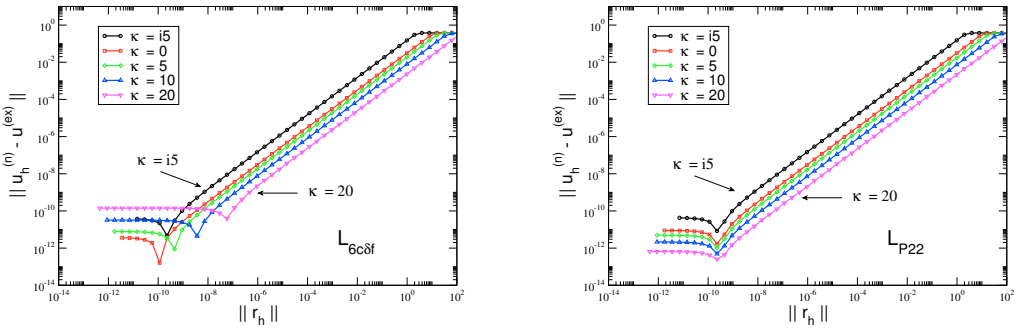

Figure 3: Discretization error $\|\boldsymbol{\epsilon}_h\|$ for the three different test cases (TC_i), explored in the present work (TC_1: $\kappa = 2$, TC_2: $\kappa = i5$, TC_3: $\kappa = 10$). In Test Case 2 the solution is split into near- and far-field part, where the near-field part has a worse error reduction due to a non-smooth source function and a singular field solution at the source origin. For comparison, also theoretical lines for the expected error behavior, $\|\boldsymbol{\epsilon}_h\| \propto h^6$, are shown.

is slightly reduced with respect to the pure schemes. Since this value of κ corresponds already to the indefinite region of the Helmholtz operator, it is not a real drawback of the schemes. Therefore the combination provides a powerful method to combine schemes of good convergence characteristics with the advantage of compactness.

3.2 Local truncation error

The order of the finite difference approximations can be checked by analysing the local truncation error τ. As an illustration this is shown explicitly here for the simple second order approximation to the Helmholtz equation, which can be written as

$$\begin{aligned}
& \frac{1}{h^2}(u(x-h,y,z)+u(x,y-h,z)+u(x,y,z-h)-6u(x,y,z) \qquad (51)\\
& \quad +u(x+h,y,z)+u(x,y+h,z)+u(x,y,z+h))-\kappa^2 u(x,y,z)+f(x,y,z)\\
= \;& \frac{1}{h^2}\left(\sum_{n=0}^{\infty}\frac{1}{n!}(\partial_x^n+\partial_y^n+\partial_z^n)u(x,y,z)(1+(-1)^n)h^n-6u(x,y,z)\right)\\
& -\kappa^2 u(x,y,z)+f(x,y,z)\\
= \;& (\partial_x^2+\partial_y^2+\partial_z^2)u(x,y,z)+\frac{h^2}{12}(\partial_x^4+\partial_y^4+\partial_z^4)u(x,y,z)-\kappa^2 u(x,y,z)+f(x,y,z)\\
= \;& (\Lambda u(x,y,z)+f(x,y,z))+\tau
\end{aligned}$$

Here, in the second part of the equation a Taylor expansion was applied to the finite difference terms. The last part shows the consistency of the approach, leading to a Helmholtz equation

plus an error, which can be written as

$$\tau = \frac{h^2}{12}(\partial_x^4 + \partial_y^4 + \partial_z^4)u(x,y,z) + \mathcal{O}(h^4) \tag{52}$$

showing that this scheme is of second order.

For the higher order schemes one finds

$$\tilde{\Lambda}_{3bl}u(x,y,z) + f(x,y,z) = S_0 + \tau_{3bl} \tag{53}$$

$$\tilde{\Lambda}_{6c}u(x,y,z)+\tilde{\Gamma}_{6c\partial f}f(x,y,z) = S_0+\frac{h^2}{12}(S_1+\kappa^2 S_0)+\frac{h^4}{360}(4S_3+S_2+\kappa^2 S_1+\kappa^4 S_0)+\tau_{6c\partial f} \tag{54}$$

$$\tilde{\Lambda}_{6c}u(x,y,z)+\tilde{\Gamma}_{6c\delta f}f(x,y,z) = S_0+\frac{h^2}{12}(S_1+\kappa^2 S_0)+\frac{h^4}{360}(4S_3+S_2+\kappa^2 S_1+\kappa^4 S_0)+\tau_{6c\delta f} \tag{55}$$

$$\tilde{\Lambda}_{P04}u(x,y,z) + \tilde{\Gamma}_{P04}f(x,y,z) = S_0 + \frac{h^2}{12}S_1 + \frac{h^4}{720}(5S_3 + 2S_2) + \tau_{P04} \tag{56}$$

$$\tilde{\Lambda}_{P22}u(x,y,z) + \tilde{\Gamma}_{P22}f(x,y,z) = S_0 + \frac{2}{15}\ h^2 S_1 + \frac{h^4}{450}(8S_3 + 5S_2) + \tau_{P22} \tag{57}$$

where the S_i are expressions which reduce to combinations of the Helmholtz equation. Due to consistency of the finite difference expressions all S_i vanish. Explicit expressions for the S_i are given in Appendix A.

The local truncation errors are thereby calculated as

$$\tau_{3bl} = \frac{1}{560}\{\partial_x^8+\partial_y^8+\partial_z^8\}u(x,y,z)\ h^6+\mathcal{O}(h^8) \tag{58}$$

$$\begin{aligned}\tau_{6c\partial f} = &\Big(\frac{1}{2160}\{\partial_x^2\partial_y^6+\partial_x^2\partial_z^6+\partial_y^2\partial_x^6+\partial_y^2\partial_z^6+\partial_z^2\partial_x^6+\partial_z^2\partial_y^6\}u(x,y,z)\\ &+\frac{1}{360}\{\partial_x^2\partial_y^2\partial_z^4+\partial_x^2\partial_z^2\partial_y^4+\partial_y^2\partial_z^2\partial_x^4\}u(x,y,z)\\ &+\frac{1}{864}\{\partial_x^4\partial_y^4+\partial_x^4\partial_z^4+\partial_y^4\partial_z^4\}u(x,y,z)+\frac{1}{20160}\{\partial_x^8+\partial_y^8+\partial_z^8\}u(x,y,z)\\ &-\frac{\kappa^2}{2160}\{\partial_x^2\partial_y^4+\partial_x^2\partial_z^4+\partial_y^2\partial_x^4+\partial_y^2\partial_z^4+\partial_z^2\partial_x^4+\partial_z^2\partial_y^4\}u(x,y,z)\Big)\ h^6+\mathcal{O}(h^8)\end{aligned} \tag{59}$$

$$\begin{aligned}\tau_{6c\delta f} = &\Big(\frac{1}{2160}S_5+\frac{1}{540}\{\partial_x^2\partial_y^2\partial_z^4+\partial_x^2\partial_z^2\partial_y^4+\partial_y^2\partial_z^2\partial_x^4\}u(x,y,z)\\ &+\frac{1}{4320}\{\partial_x^4\partial_y^4+\partial_x^4\partial_z^4+\partial_y^4\partial_z^4\}u(x,y,z)+\frac{1}{20160}\{\partial_x^8+\partial_y^8+\partial_z^8\}u(x,y,z)\\ &+\frac{1}{2160}\{\partial_x^2\partial_y^4+\partial_x^2\partial_z^4+\partial_y^2\partial_x^4+\partial_y^2\partial_z^4+\partial_z^2\partial_x^4+\partial_z^2\partial_y^4\}f(x,y,z)\\ &-\frac{1}{2160}\{\partial_x^6+\partial_y^6+\partial_z^6\}f(x,y,z)+\frac{\kappa^2}{4320}\{\partial_x^4+\partial_y^4+\partial_z^4\}f(x,y,z)\Big)\ h^6+\mathcal{O}(h^8)\end{aligned} \tag{60}$$

$$\begin{aligned}\tau_{P04} = &\Big(\frac{1}{1728}S_5-\frac{1}{2160}S_4+\frac{1}{1728}\{\partial_x^2\partial_y^2\partial_z^4+\partial_x^2\partial_z^2\partial_y^4+\partial_y^2\partial_z^2\partial_x^4\}u(x,y,z)\\ &-\frac{1}{1440}\{\partial_x^4\partial_y^4+\partial_x^4\partial_z^4+\partial_y^4\partial_z^4\}u(x,y,z)\\ &-\frac{1}{2880}\{\partial_x^2\partial_y^6+\partial_x^2\partial_z^6+\partial_y^2\partial_x^6+\partial_y^2\partial_z^6+\partial_z^2\partial_x^6+\partial_z^2\partial_y^6\}u(x,y,z)\\ &+\frac{17}{20160}\{\partial_x^8+\partial_y^8+\partial_z^8\}u(x,y,z)\Big)\ h^6+\mathcal{O}(h^8)\end{aligned} \tag{61}$$

$$\begin{aligned}\tau_{P22} = &\Big(\frac{1}{675}S_5+\frac{1}{2700}S_4\\ &+\frac{1}{675}\{\partial_x^2\partial_y^2\partial_z^4+\partial_x^2\partial_z^2\partial_y^4+\partial_y^2\partial_z^2\partial_x^4\}u(x,y,z)\\ &+\frac{23}{75600}\{\partial_x^8+\partial_y^8+\partial_z^8\}u(x,y,z)\Big)\ h^6+\mathcal{O}(h^8)\end{aligned} \tag{62}$$

Another way to verify the order of the approximations is to apply the finite difference schemes to the sampled eigenfunctions of the continuous operators. Since the *rhs* of the Helmholtz equation is modified in the cases of L_{6c}, L_{P04} and L_{P22} a generalized eigenvalue problem has to be considered. Complimentary to the present analysis, the eigenvalue method is shown in Appendix B.

3.3 Test cases

In this section several case studies are presented for the Helmholtz equation. Results are compared to analytical solutions. All test cases were run on an IBM T30 notebook with a 2 GHz Pentium IV processor with 1 GB DRAM. The program is implemented in Fortran 90 and translated with the Intel compiler version 8.0.

3.3.1 Test Case 1

A straight forward choice as a test is using a sampled eigenfunction of the Laplace operator

$$u_{i,j,k} = \sin(\pi i h_x/L)\sin(\pi j h_y/L)\sin(\pi k h_z/L) \tag{63}$$

from where the source function is given as

$$f_{i,j,k} = (3\pi^2/L^2 + \kappa^2)\sin(\pi i h_x/L)\sin(\pi j h_y/L)\sin(\pi k h_z/L) \tag{64}$$

For practical purposes the length L of the box was normalized, $L = 1$.

3.3.2 Test Case 2

Depending on the sign of κ^2, this test case consists of either e.g. calculating the electrostatic potential of a point charge in an electrolyte solution ($\kappa^2 > 0$), or e.g. the propagtion of a wave due to a point source ($\kappa^2 < 0$), i.e. the source function is given by

$$f(\mathbf{r}) = 4\pi\delta(\mathbf{r}-\mathbf{r}_0) \qquad \rightarrow \qquad f_{i,j,k} = \begin{cases} \dfrac{4\pi}{h_x h_y h_z} & : \quad (x = ih_x, y = jh_y, z = kh_z) = 0.5 \\ 0 & : \quad \text{else} \end{cases} \tag{65}$$

which has the analytical solution for the field

$$u(\mathbf{r}) = \frac{e^{-\kappa|\mathbf{r}-\mathbf{r}_0|}}{|\mathbf{r}-\mathbf{r}_0|} \tag{66}$$

3.3.3 Test Case 3

This test case was taken from Ref. [3] and extended to three dimensions. The potential function is given by

$$u_{i,j,k} = \frac{1}{\cosh(10)}\left(\cosh(10ih_x)\cosh(10jh_y)\cosh(10kh_z)\right) \tag{67}$$

with $\kappa = 10$, i.e. the source function vanishes, $f_{i,j,k} = 0$.

Results for all test cases in terms of the discretization error are shown in Fig. 4. In each case the predicted behavior of error reduction, i.e. $\|\boldsymbol{\epsilon}_h\| \propto h^6$, is found. The only special case is observed for Test Case 2, where the solution is subdivided into a near- and far-field contribution. As a convention the near field part is defined here via the spatial resolution of the coarsest grid with $h = 1/8$, i.e. $u_{ijk}^{(near)} = u_{ijk}(r|\alpha \in [3/8, 5/8], \alpha = x, y, z)$ and $u_{ijk}^{(far)} = u_{ijk}(r|\alpha \notin [3/8, 5/8], \alpha = x, y, z)$. The point source function produces a solution which is non-smooth close to the source and therefore the solution of a relaxation procedure gives rather poor results in this region. It is found that the error reduction in the near-field part is only $\propto h^{0.4}$. This is mainly due to nearest grid points close to the point source, where the analytical solution of the potential diverges, i.e. the finer the grid the faster the solution should get larger values at these grid points. It is found empirically that the error close to the source remains more or less constant, so that the overall error reduction is due to those

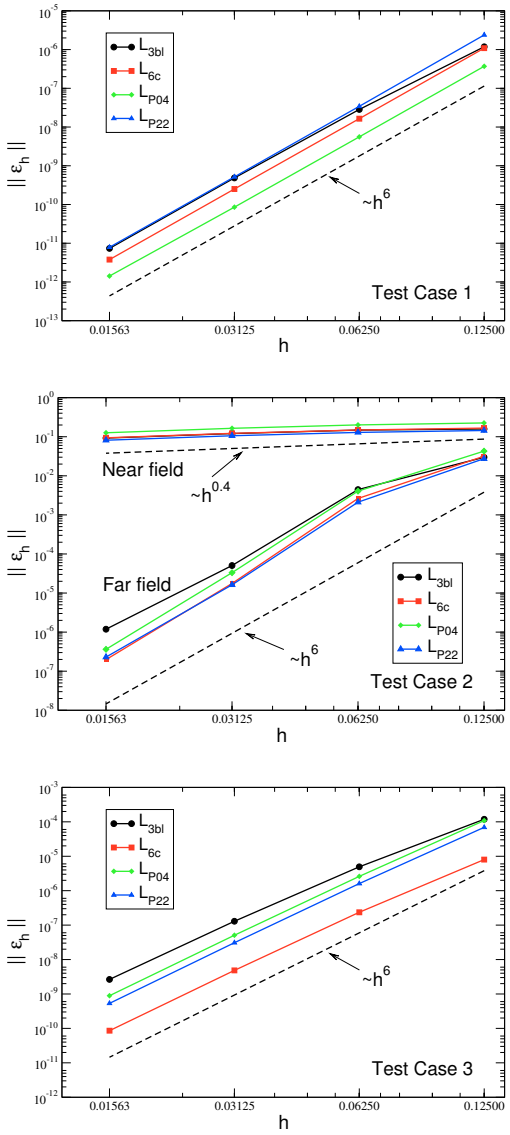

Figure 4: Discretization error $\|\boldsymbol{\epsilon}_h\|$ for the three different test cases (TC_i), explored in the present work (TC_1: $\kappa = 2$, TC_2: $\kappa = i5$, TC_3: $\kappa = 10$). In Test Case 2 the solution is split into near- and far-field part, where the near-field part has a worse error reduction due to a non-smooth source function and a singular field solution at the source origin. For comparison, also theoretical lines for the expected error behavior, $\|\boldsymbol{\epsilon}_h\| \propto h^6$, are shown.

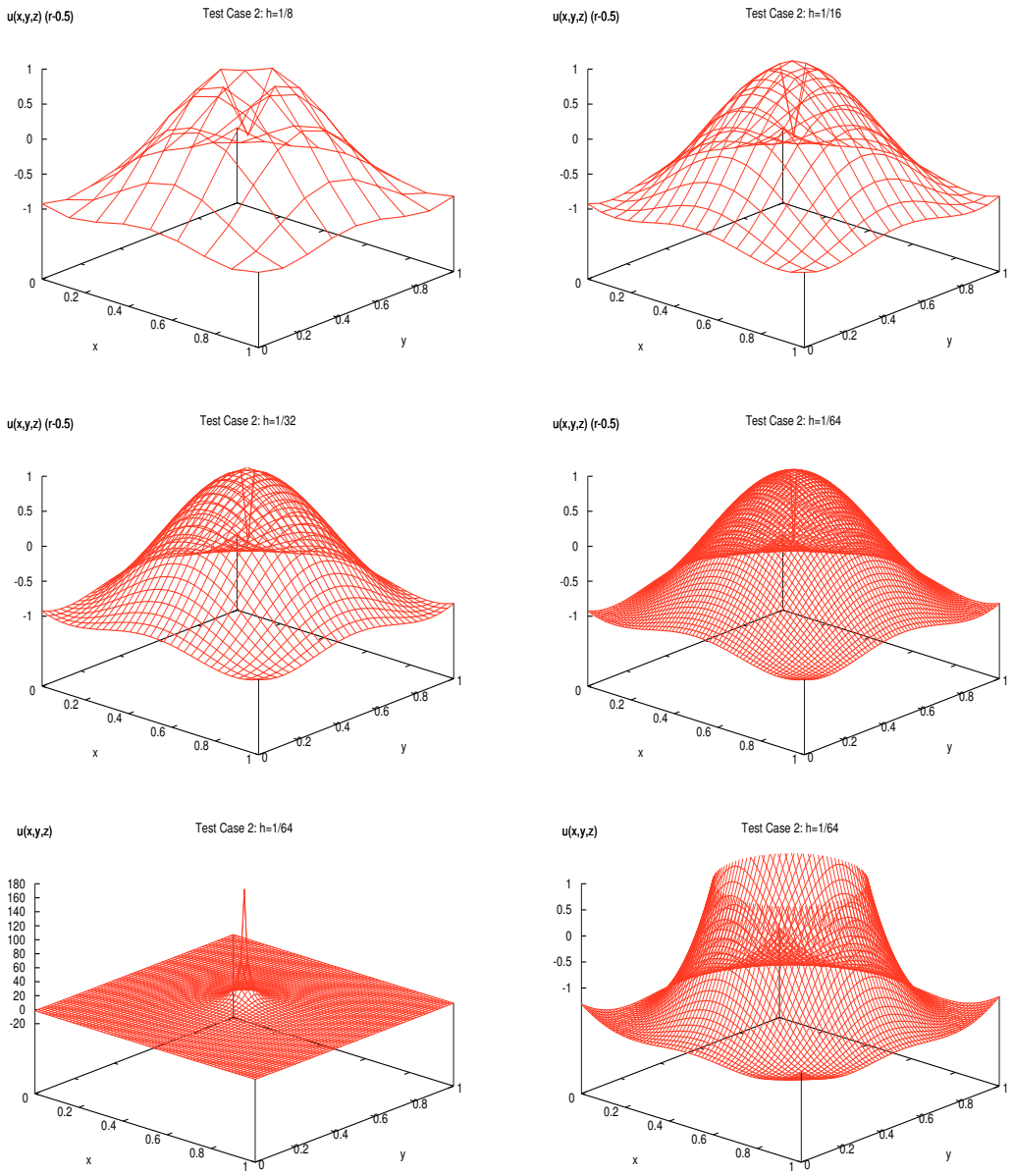

Figure 5: Representation of the solution of Test Case 3 with $\kappa = i5$ on different grid sizes. In the upper four figures it is shown $u(x, y, z) \times (\mathbf{r} - 0.5\,\mathbf{1})$ which corresponds to an exponentially damped wave. The two lower figures show the full solution on the grid $h = 1/64$ and a detailed view, cut at $u(x, y, z) = 1$. All figures correspond to a cut through the (x, y)-plane at $z = 0.5$.

points in the outer region of the near field where the solution already behaves smoother. On the other hand, the far field part of the potential shows the expected error reduction due to the fact that the field is smooth and well behaved. A cut at $z = 1/2$ shows the solution of Test Case 2 in the x-y-plane for $\kappa = i5$ for four different mesh sizes. For a better view on the infrastructure of the solution, also $u(x, y, z) \times (\mathbf{r} - \mathbf{1}/2)$ is shown, where $\mathbf{1}$ is a unit vector in (x, y, z)-direction.

4 Conclusions

Finite difference schemes of sixth order were derived and applied to a set of different test cases on grids with mesh spacings in the range $h \in [1/64, 1/8]$. The new schemes have advantages and disadvantages when considered individually. For example, the schemes based on the Padé approximations both need next nearest grid points in the iteration matrix, introducing problems at the boundary of the computational domain, if only one layer of boundary layers is known in the Dirichlet problem (which is usually the case). On the other hand these solvers have good convergence characteristics and small discretization errors. In contrast, the proposed scheme $L_{6c\partial f}$ only need one boundary layer for both the *lhs* and *rhs* of the Helmholtz equation. This is true if the source function is sufficiently differentiable. Otherwise a discrete finite difference scheme has to be applied to the *rhs* needing two neighboured grid points. This may introduce again problems at the domain boundary. It was found that the scheme $L_{6c\partial f}$, although having an analytical derivative on the *rhs* exhibits a worse discretization error than $L_{6c\delta f}$. Therefore a compromise was suggested to combine those schemes which require next nearest grid points ($L_{6c\delta f}$, L_{P04}, L_{P22}) with $L_{6c\partial f}$, where the former schemes are applied in the interior of the domain and the latter one close to the boundary, leading to the schemes $L_{6c\delta f/6c\partial f}$, $L_{P04/6c\partial f}$, $L_{P22/6c\partial f}$. Especially in the case of the Padé schemes the good convergence characteristics as well as the small discretization error are conserved, so that these schemes lead to high order procedures for a big class of problems. The computational overhead introduced by mixing different schemes seems to be negligible from the present investigations. It may be noted that mixed schemes can be avoided in the case where periodic boundary conditions are applied or where the distribution of the source function vanishes near to the boundary. These cases appear e.g. in the context of molecular simulations, where charged particles are located in the centre of the computational domain [9].

Acknowledgments

The author is very grateful to B. Steffen for interesting and stimulating discussions. Also discussions with J. Grotendorst and T. Holtschneider are acknowledged.

A Expressions for the S_i

The basic expression for the S_i is the bare Helmholtz equation

$$S_0 = \Lambda u(x, y, z) + f(x, y, z) = 0 \tag{68}$$

Applying partial derivatives and summing up terms, one gets the following expressions for higher S_i

$$
\begin{aligned}
S_1 &= \{\partial_x^2+\partial_y^2+\partial_z^2\}\ S_0 && (69)\\
&= \{\partial_x^2\partial_y^2+\partial_x^2\partial_z^2+\partial_y^2\partial_z^2\}\ u(x,y,z)+\{\partial_x^4+\partial_y^4+\partial_z^4\}\ u(x,y,z)\\
&\quad -\kappa^2\{\partial_x^2+\partial_y^2+\partial_z^2\}\ u(x,y,z)+\{\partial_x^2+\partial_y^2+\partial_z^2\}\ f(x,y,z)\\
S_2 &= \{\partial_x^4+\partial_y^4+\partial_z^4\}\ S_0 && (70)\\
&= \{\partial_x^2\partial_y^4+\partial_x^2\partial_z^4+\partial_y^2\partial_x^4+\partial_y^2\partial_z^4+\partial_z^2\partial_x^4+\partial_z^2\partial_y^4\}\ u(x,y,z)\\
&\quad +\{\partial_x^6+\partial_y^6+\partial_z^6\}\ u(x,y,z)-\kappa^2\{\partial_x^4+\partial_y^4+\partial_z^4\}\ u(x,y,z)\\
&\quad +\{\partial_x^4+\partial_y^4+\partial_z^4\}\ f(x,y,z)=0\\
S_3 &= \{\partial_x^2\partial_y^2+\partial_x^2\partial_z^2+\partial_y^2\partial_z^2\}\ S_0 && (71)\\
&= \{\partial_x^2\partial_y^4+\partial_x^2\partial_z^4+\partial_y^2\partial_x^4+\partial_y^2\partial_z^4+\partial_z^2\partial_x^4+\partial_z^2\partial_y^4\}\ u(x,y,z)\\
&\quad +3\partial_x^2\partial_y^2\partial_z^2\ u(x,y,z)-\kappa^2\{\partial_x^2\partial_y^2+\partial_x^2\partial_z^2+\partial_y^2\partial_z^2\}\ u(x,y,z)\\
&\quad +\{\partial_x^2\partial_y^2+\partial_x^2\partial_z^2+\partial_y^2\partial_z^2\}\ f(x,y,z)=0\\
S_4 &= \{\partial_x^6+\partial_y^6+\partial_z^6\}\ S_0 && (72)\\
&= \{\partial_x^2\partial_y^6+\partial_x^2\partial_z^6+\partial_y^2\partial_x^6+\partial_y^2\partial_z^6+\partial_z^2\partial_x^6+\partial_z^2\partial_y^6\}\ u(x,y,z)\\
&\quad +\{\partial_x^8+\partial_y^8+\partial_z^8\}\ u(x,y,z)-\kappa^2\{\partial_x^6+\partial_y^6+\partial_z^6\}\ u(x,y,z)\\
&\quad +\{\partial_x^6+\partial_y^6+\partial_z^6\}\ f(x,y,z)=0\\
S_5 &= \{\partial_x^2\partial_y^4+\partial_x^2\partial_z^4+\partial_y^2\partial_x^4+\partial_y^2\partial_z^4+\partial_z^2\partial_x^4+\partial_z^2\partial_y^4\}\ S_0 && (73)\\
&= \{\partial_x^2\partial_y^6+\partial_x^2\partial_z^6+\partial_y^2\partial_x^6+\partial_y^2\partial_z^6+\partial_z^2\partial_x^6+\partial_z^2\partial_y^6\}\ u(x,y,z)\\
&\quad +2\{\partial_x^4\partial_y^4+\partial_x^4\partial_z^4+\partial_y^4\partial_z^4\}\ u(x,y,z)\\
&\quad +2\{\partial_x^2\partial_y^2\partial_z^4+\partial_x^2\partial_z^2\partial_y^4+\partial_y^2\partial_z^2\partial_x^4\}\ u(x,y,z)\\
&\quad -\kappa^2\{\partial_x^2\partial_y^4+\partial_x^2\partial_z^4+\partial_y^2\partial_x^4+\partial_y^2\partial_z^4+\partial_z^2\partial_x^4+\partial_z^2\partial_y^4\}\ u(x,y,z)\\
&\quad +\{\partial_x^2\partial_y^4+\partial_x^2\partial_z^4+\partial_y^2\partial_x^4+\partial_y^2\partial_z^4+\partial_z^2\partial_x^4+\partial_z^2\partial_y^4\}\ f(x,y,z)=0
\end{aligned}
$$

B Operator expansions

In order to validate formally the order of the proposed operators, expansions in terms of grid spacings, h, were applied to the generalized eigenvalue problem

$$\left(\tilde{\Lambda}\phi_{klm}-(k^2+l^2+m^2+\kappa^2)\tilde{\Gamma}\phi_{klm}\right)\ \phi_{klm}^{-1}=\mathcal{O}(h^n) \tag{74}$$

where n gives the order of the approximation, ϕ is an eigenfunction, $\tilde{\Lambda}$ is the approximate Helmholtz operator

$$\tilde{\Lambda}=\tilde{\Delta}_h^{(n)}-\kappa^2 \tag{75}$$

and $\tilde{\Delta}_h^{(n)}$ is an approximation to the Laplace operator of order n.

An appropriate eigenfunction is simply chosen as

$$\phi_{klm}(x,y,z) = \cos(kx)\cos(ly)\cos(mz) \tag{76}$$

Applying the finite difference operators gives the following expansions $\mathcal{E}$

$$\mathcal{E}\{\Lambda_{3bl}\} = \frac{1}{560}\left(k^8+l^8+m^8\right)h^6 + \mathcal{O}(h^8) \tag{77}$$

$$\begin{aligned}\mathcal{E}\{\Lambda_{6c\partial f}\} &= \frac{1}{360}\left(k^2l^2m^4+l^2m^2k^4+m^2k^2l^4\right)\,h^6 \\ &+\frac{1}{2160}\left(k^2(l^4+m^4)+l^2(k^4+m^4)+m^2(k^4+l^4)\right)\,h^6 \\ &+\frac{1}{864}\left(k^4l^4+k^4m^4+l^4m^4\right)\,h^6+\frac{1}{20160}\left(k^8+l^8+m^8\right)\,h^6 \\ &+\frac{\kappa^2}{2160}\left(k^2(l^4+m^4)+l^2(k^4+m^4)+m^2(k^4+l^4)\right)\,h^6+\mathcal{O}(h^8)\end{aligned} \tag{78}$$

$$\begin{aligned}\mathcal{E}\{\Lambda_{6c\delta f}\} &= \frac{1}{1080}\left(k^2l^2m^4+l^2m^2k^4+m^2k^2l^4\right)\,h^6 \\ &-\frac{1}{1440}\left(k^4l^4+k^4m^4+l^4m^4\right)\,h^6 \\ &+\frac{31}{60480}\left(k^8+l^8+m^8\right)\,h^6 \\ &-\frac{\kappa^2}{2160}\Big(k^2(l^4+m^4)+l^2(k^4+m^4)+m^2(k^4+l^4) \\ &+k^6+l^6+m^6\Big)\,h^6+\mathcal{O}(h^8)\end{aligned} \tag{79}$$

$$\begin{aligned}\mathcal{E}\{\Lambda_{P04}\} &= \frac{1}{1728}\left(k^2l^2m^4+k^2l^4m^2+k^4l^2m^2\right)\,h^6 \\ &-\frac{1}{1440}\left(k^4l^4+k^4m^4+l^4m^4\right)\,h^6 \\ &-\frac{1}{2880}\left(k^6(l^2+m^2)+l^6(k^2+m^2)+m^6(k^2+l^2)\right)\,h^6 \\ &+\frac{31}{60480}\left(k^8+l^8+m^8\right)\,h^6+\mathcal{O}(h^8)\end{aligned} \tag{80}$$

$$\begin{aligned}\mathcal{E}\{\Lambda_{P22}\} &= \frac{1}{675}\left(k^2l^2m^4+k^2l^4m^2+k^4l^2m^2\right)\,h^6 \\ &+\frac{23}{75600}\left(k^8+l^8+m^8\right)\,h^6+\mathcal{O}(h^8)\end{aligned} \tag{81}$$

Some graphical representations of the operator expansions for $k=1$ are shown in Fig. 6. Note the expansions of operators $\Lambda_{6c\partial f}$ and $\Lambda_{6c\delta f}$. In the case where finite difference approximations to the derivatives of the *rhs* are applied ($\Lambda_{6c\delta f}$) there are alternating signs in the expansion while the case where the *rhs* is differentiated analytically, only positive signs appear. This leads to an overall larger truncation error in the expansion. In fact, calculating the sum

$$\varepsilon_\Lambda(K) = \sum_{k,l,m}^{K}\mathcal{E}\{\Lambda\}(k,l,m) \tag{82}$$

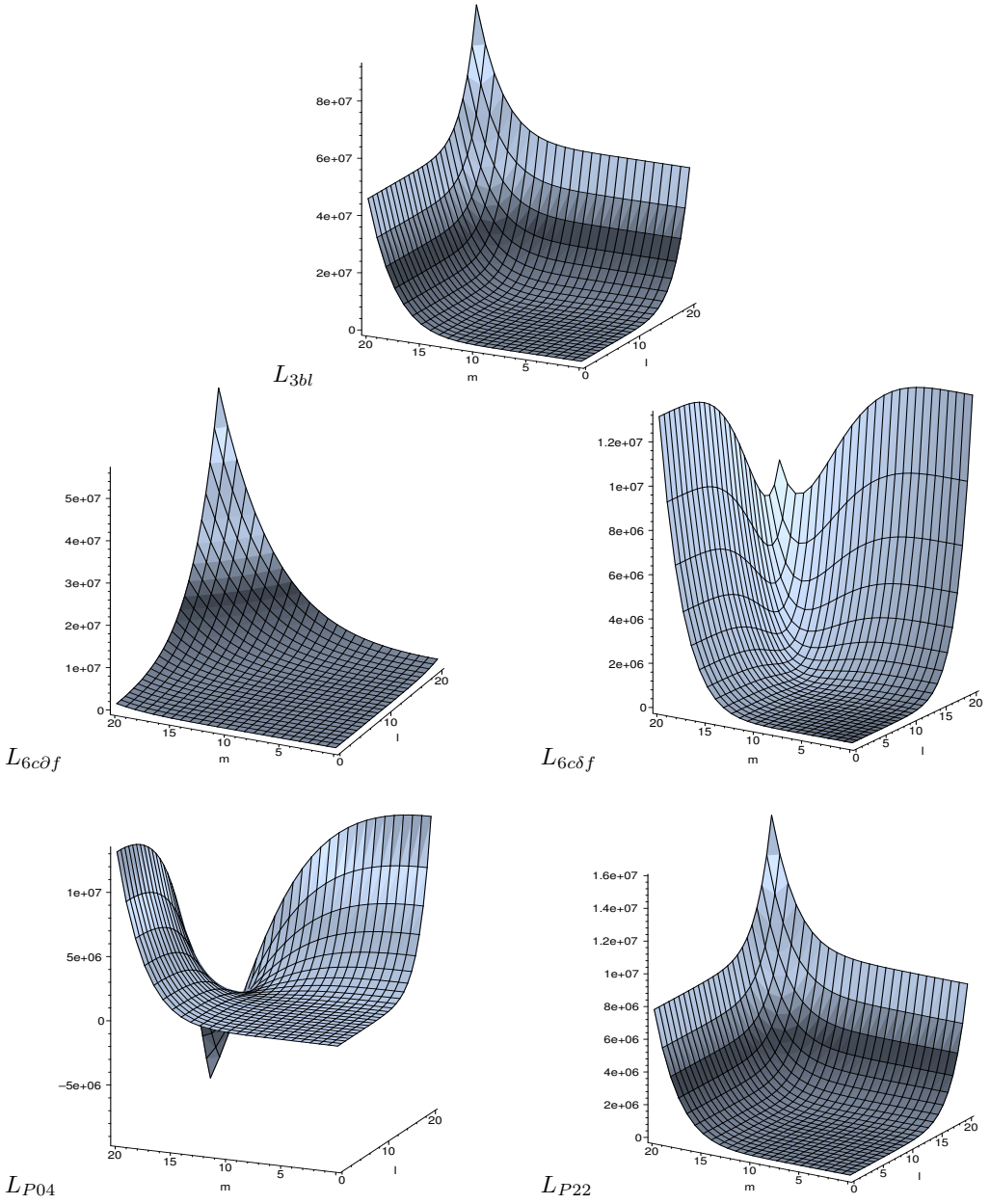

Figure 6: Sixth order error behavior of the eigenvalue method for finite difference schemes L_{3bl}, $L_{6c\partial f}$, $L_{6c\delta f}$, L_{P04} and L_{P22} for $k = 1$. In the case of $L_{6c\partial f}$ and $L_{6c\delta f}$, $\kappa = 0$.

it is found that $\varepsilon_{\Lambda_{6c\partial f}}(K)/\varepsilon_{\Lambda_{6c\delta f}}(K) > 3$ for all K, showing that one has to expect a larger truncation error for $\Lambda_{6c\partial f}$ than for $\Lambda_{6c\delta f}$.

C Maple module for finite difference operators

Here a Maple module is shown, which constructs finite difference operators for even derivatives [10]. All schemes are derived from the forward and backward shift operators

$$\delta_{f,x} u_h \equiv u(x+h,y,z) - u(x,y,z) \tag{83}$$
$$\delta_{b,x} u_h \equiv u(x,y,z) - u(x-h,y,z) \tag{84}$$

For other dimensions it follows analogously.

```
> FiniteDifference := module()

  export dfx, dfy, dfz, dbx, dby, dbz,
         d2x, d2y, d2z, d4xx, d4yy, d4zz, d4xy, d4xz, d4yz,
         d6xxx, d6yyy, d6zzz, d6xyy, d6xzz,
         d6yxx, d6yzz, d6zxx, d6zyy, d6xyz,
         D0, D2, D22, D4, D222, D24, D6;

Forward and Backward shift operators

> dfx := f -> ((h) -> f(x+h,y,z)-f(x,y,z));
> dfy := f -> ((h) -> f(x,y+h,z)-f(x,y,z));
> dfz := f -> ((h) -> f(x,y,z+h)-f(x,y,z));
> dbx := f -> ((h) -> f(x,y,z)-f(x-h,y,z));
> dby := f -> ((h) -> f(x,y,z)-f(x,y-h,z));
> dbz := f -> ((h) -> f(x,y,z)-f(x,y,z-h));

Approximation of 2nd derivatives

> d2x := f -> ((h) -> dfx(unapply(dbx(f)(h),x,y,z))(h));
> d2y := f -> ((h) -> dfy(unapply(dby(f)(h),x,y,z))(h));
> d2z := f -> ((h) -> dfz(unapply(dbz(f)(h),x,y,z))(h));

Approximation of 4th derivatives

> d4xx := f -> ((h) -> d2x(unapply(d2x(f)(h),x,y,z))(h));
> d4yy := f -> ((h) -> d2y(unapply(d2y(f)(h),x,y,z))(h));
> d4zz := f -> ((h) -> d2z(unapply(d2z(f)(h),x,y,z))(h));
> d4xy := f -> ((h) -> d2y(unapply(d2x(f)(h),x,y,z))(h));
> d4xz := f -> ((h) -> d2z(unapply(d2x(f)(h),x,y,z))(h));
> d4yz := f -> ((h) -> d2z(unapply(d2y(f)(h),x,y,z))(h));

Approximation of 6th derivatives
```

```
> d6xxx := f -> ((h) -> d2x(unapply(d4xx(f)(h),x,y,z))(h));
> d6yyy := f -> ((h) -> d2y(unapply(d4yy(f)(h),x,y,z))(h));
> d6zzz := f -> ((h) -> d2z(unapply(d4zz(f)(h),x,y,z))(h));
> d6xyy := f -> ((h) -> d2x(unapply(d4yy(f)(h),x,y,z))(h));
> d6xzz := f -> ((h) -> d2x(unapply(d4zz(f)(h),x,y,z))(h));
> d6yxx := f -> ((h) -> d2y(unapply(d4xx(f)(h),x,y,z))(h));
> d6yzz := f -> ((h) -> d2y(unapply(d4zz(f)(h),x,y,z))(h));
> d6zxx := f -> ((h) -> d2z(unapply(d4xx(f)(h),x,y,z))(h));
> d6zyy := f -> ((h) -> d2z(unapply(d4yy(f)(h),x,y,z))(h));
> d6xyz := f -> ((h) -> d2x(unapply(d4yz(f)(h),x,y,z))(h));

Composite expressions for three dimensional finite difference approximations

> D0 := f -> ((h) -> f(x,y,z));
> D2 := f -> ((h) -> d2x(f)(h) + d2y(f)(h) + d2z(f)(h));
> D22 := f -> ((h) -> d4xy(f)(h) + d4xz(f)(h) + d4yz(f)(h));
> D24 := f -> ((h) -> d6xyy(f)(h) + d6xzz(f)(h) + d6yxx(f)(h)
                    + d6yzz(f)(h) + d6zxx(f)(h) + d6zyy(f)(h));
> D222 := f -> ((h) -> d6xyz(f)(h));
> D4 := f -> ((h) -> d4xx(f)(h) + d4yy(f)(h) + d4zz(f)(h));
> D6 := f -> ((h) -> d6xxx(f)(h) + d6yyy(f)(h) + d6zzz(f)(h));

end module;
```

As an example consider the *rhs* of the Helmholtz equation as derived in the $\mathcal{P}[0,4]$ approximation

```
> with(FiniteDifference):
> D0(f)(h)+2/15*D2(f)(h)+4/225*D22(f)(h);
  31              14                    14
  -- f(x, y, z) + --- f(x - h, y, z) + --- f(x + h, y, z)
  75              225                   225
            14                    14
          + --- f(x, y - h, z) + --- f(x, y + h, z)
            225                   225
            14                    14
          + --- f(x, y, z - h) + --- f(x, y, z + h)
            225                   225
          + 4/225 f(x + h, y - h, z) + 4/225 f(x - h, y - h, z)
          + 4/225 f(x + h, y + h, z) + 4/225 f(x - h, y + h, z)
          + 4/225 f(x + h, y, z - h) + 4/225 f(x - h, y, z - h)
          + 4/225 f(x + h, y, z + h) + 4/225 f(x - h, y, z + h)
          + 4/225 f(x, y + h, z - h) + 4/225 f(x, y - h, z - h)
          + 4/225 f(x, y + h, z + h) + 4/225 f(x, y - h, z + h)
```

References

[1] E. N. Houstis and T. S. Papatheodorou. In R. Vichnevetsky, editor, *Advances in Computer Methods for Partial Differential Equations*, volume II, pages 46–52, New Brunswick, N.J., 1977. IMACS.

[2] R. F. Boisvert. *SIAM J. Sci. Stat. Comput.*, 2:268, 1981.

[3] R. P. Manohar and J. W. Stephenson. Single cell high order difference methods for the Helmholtz equation. *J. Comp. Phys..*, 51:444–453, 1983.

[4] I. Harari and E. Turkel. Accurate finite difference methods for time-harmonic wave propagation. *J. Comp. Phys..*, 119:252–270, 1995.

[5] I. Singer and E. Turkel. High-order finite difference methods for the Helmholtz equation. *Comput. Meth. Appl. Mech. Engrg.*, 163:343–358, 1998.

[6] G. Sutmann and B. Steffen. High-order compact solvers for the three dimensional Poisson equation. J. Comp. Appl. Math. (in press).

[7] W. F. Ames. *Numerical Methods for Partial Differential Equations.* Academic Press, New York, 1977.

[8] W. F. Spotz and G. F. Carey. A high-order compact formulation for the 3d Poisson equation. *Num. Meth. Part. Diff. Equat.*, 12:235–243, 1996.

[9] G. Sutmann and B. Steffen. A particle-particle particle-multigrid method for long-range interactions in molecular simulations. Comp. Phys. Comm. 169:343–346, 2005.

[10] The module may be downloaded from http://www.fz-juelich.de/zam/cams/HOC